

OPEN

Demonstration of facilitation between microalgae to face environmental stress

Emna Krichen^{1,2,3}, Alain Rapaport², Emilie Le Floc'h¹ & Eric Fouilland^{1*}

Positive interactions such as facilitation play an important role during the biological colonization and species succession in harsh or changing environments. However, the direct evidence of such ecological interaction in microbial communities remains rare. Using common freshwater microalgae isolated from a High Rate Algal Pond *HRAP* treating wastewaters, we investigated with both experimental and modeling approaches the direct facilitation between two algal strains during the colonization phase. Our results demonstrate that the first colonization by microalgae under a severe chemical condition arose from the rapid growth of pioneer species such as *Chlorella sorokiniana*, which facilitated the subsequent colonization of low growth specialists such as *Scenedesmus pectinatus*. The pioneer species rapidly depleted the total available ammonia nitrogen favoring the specialist species initially inhibited by free ammonia toxicity. This latter species ultimately dominated the algal community through competitive exclusion under low nutrient conditions. We show that microbial successions are not only regulated by climatic conditions but also by interactions between species based on the ability to modify their growth conditions. We suggest that facilitation within the aquatic microbial communities is a widespread ecological interaction under a vast range of environmental stress.

One of the major challenges in microbial ecology is to understand the dynamics of communities of interacting species. Understanding the biological interactions and the time scales over which they occur is necessary to interpret the results of the directional succession process of communities' development in the natural environment and artificial ecosystems. In aquatic systems, microalgae are present in natural waters such as oceans, lakes, rivers, and ponds and play a prominent role in the marine and fresh-water ecosystems where they drive major ecosystem processes. Strong similarities exist between marine and freshwater phytoplankton ecology¹ when they face similar changes in growth conditions leading to temporal species succession. Abiotic forcing and biotic interactions can both result in successional trends in phytoplankton. The scientific discussion around the phytoplankton growth periodicity and succession has been dominated by the role of the environmental drivers including global climatic change (e.g. light, temperature, wind)^{2–6} local hydrological variations^{7,8} biological disturbances such as species invasion⁹, and chemical effects such as toxic pollutants, nutrient enrichment, or change in *pH* (see references^{6,7,10–12}). On the other hand, the conditions governing phytoplankton growth over the seasonal change in plankton communities have mostly been discussed in the context of exploitative competition (e.g. Tilman, 1982)¹³ or algae-grazer interactions (e.g. Porter, 1977)¹⁴.

The competition for limiting nutrients is an important factor explaining phytoplankton species temporal successions. In marine ecosystems, small-cell diatoms usually grow rapidly in the first stage after a strong nutrient enrichment because of their higher growth rates and are then followed by larger-cell diatoms and dinoflagellates, which are more likely to occur when nutrients are depleted^{15,16}. Similarly, the seasonal patterns of succession in freshwater ecosystems might be explained by the first occurrence of invasive small-sized species¹⁷, which can be expected to continue to expand until they either run out of nutrient or light energy or are controlled by zooplankton grazing^{17,18}. These pioneer invasive species can be replaced by other phytoplankton species more prone to grow under nutrient depletion because of mixotrophy ability or mobility allowing them to exploit patches of nutrients not available to other microalgae¹⁷.

The ability to colonize a specific habitat usually explains the dominance and succession under changes in environmental conditions. For instance, changes in the algal assemblage in natural biofilm communities have been

¹MARBECC, Univ. Montpellier, CNRS, IFREMER, IRD, Sète, France. ²MISTEA, Univ. Montpellier, INRA, SupAgro, Montpellier, France. ³ADEME, Agence de l'environnement et de la Maîtrise de l'Energie, 20 avenue du Grésillé, BP 90406, 49004 Angers Cedex 01, France. *email: eric.fouilland@cnrs.fr

reported in the context of ecological succession that may be related to the population's tolerance to the physical architecture of the developing mat or the resource limitations within the mat occurring as the biofilm develops¹⁹.

Positive interactions (i. e. facilitation) between organisms can occur when one organism makes the local environment more favorable for another either directly (such as by reducing thermal, water or nutrient stress via shading or through nutritional symbioses) or indirectly (such as by removing competitors or deterring predators)²⁰. Positive feedbacks are the main driving biotic mechanism in plant community succession, particularly under harsh environmental conditions including physical or biotic stresses²¹ and are potentially important in aquatic systems influencing the dynamics of populations and communities^{19,20}. However, fewer studies have discussed the role of positive interactions in aquatic microbial communities' organizations. During the biofilm development, it was suggested that early stages of diatoms succession follow the "facilitation" model outlined by Connell and Slatyer²² when the extracellular mucilage production modified the physical biofilm characteristics and then enhanced the probability of successful immigration of some species more than others²³. Similarly, it was suggested that algal mucilage and stalks within the biofilm facilitate periphyton development by encouraging cell surface adhesion and providing increased sites for colonization²⁴.

Phytoplankton can substantially change its surrounding conditions of growth by increasing *pH* due to the uptake of inorganic carbon during photosynthesis²⁵, decreasing transparency with the increase of biomass concentration²⁶ or depleting key nutrients. Hence, we suggest that this phytoplankton-driven environmental modification can provoke shifts in assemblages of species, thus leading to successions. We suppose that under highly polluted conditions, similar to strongly anthropized ecosystems, an assemblage of typical pioneer species will first develop because of their potential for rapid dispersal and growth. We hypothesize that species showing the fastest growth rates and the strongest stress tolerance to harsh environments will be able to grow under such conditions, making the ecosystem more favorable for species that are more competitive in stable growth conditions through ecological facilitation.

Previous results from a study investigating the biological succession within HRAPs used for wastewater treatment showed the growth of the rapid-growing species *Chlorella* sp. followed by the slow-growing and grazing-resilient species *Scenedesmus* sp.²⁷. Similar successions have been observed in other studies using HRAPs as well^{28,29}. The successional trends of typical microalgal species growing in HRAPs have generally been interpreted as responses to predation and/or seasonal factors^{28,30}. Based on the previous observations of dominant species dynamics²⁷, we tested in this study the hypothesis that during the colonization phase of HRAPs supplemented with wastewaters, *Chlorella* sp. can modify its habitat and facilitate the growth conditions for *Scenedesmus* sp. by reducing the nutrient stress modulated by ammonia toxicity³¹. We suggest that microbial successions might not be regulated by climatic conditions only, but also through positive interactions between species facing external chemical stress. We conducted sets of laboratory experiments using the species molecularly identified as *C. sorokiniana* and *S. pectinatus* on isolates taken from the HRAP located in northern France during its colonization by *Chlorella* sp. and *Scenedesmus* sp. being both previously identified by microscopy²⁷. The objectives of these experiments were to determine the inhibiting factor among ammonium ion NH_4^+ , *pH* and free ammonia NH_3 and to determine their respective effects on the growth rates of each species. Then, we used a modeling approach to test the magnitude of facilitation/competition on the two microalgae and, further, to explain the observed patterns in HRAP continuously supplemented with wastewater²⁷. We also studied the resilience and succession times, providing informative proxies on the efficiency of the ecological facilitation and the successional trends depending on the initial populations' densities. Our results supported the theoretical considerations of ecological facilitation between one tolerant and one sensitive organism to a gradient of resource toxicity/bioavailability.

Results and Discussion

Three sets of experiments (denoted SE1, SE2 and SE3) were performed (i) to isolate the inhibitory effects of possible external factors such as high nitrogen concentrations or *pH* and (ii) to demonstrate a facilitation interaction between two species. We then show how to exploit the experimental data using a mathematical modeling approach, providing new insights on the facilitation phenomenon.

No direct toxic effect of high NH_4^+ and *pH* on microalgae growth rates. Chemical factors such as Total Ammonia Nitrogen TAN and *pH* can affect the rate and efficiency of photosynthesis of microalgae^{32–34}. Negative effects of TAN (referring to nitrogen in two distinct forms: NH_4^+ and NH_3 on algal growth and physiology might occur and vary significantly within classes of microalgae and within species (see³⁵). The photosynthesis of different species of marine diatoms was severely inhibited at TAN concentrations in the range of 0.5 to 11 $mgN.L^{-1}$ (see^{36,37}). At low *pH* values (<8), toxicity is likely associated with NH_4^+ , while at alkaline *pH* values (>8), cell growth inhibition is rather due to NH_3 . During the first set of experiments SE1, the potential toxicity of high NH_4^+ was investigated for the two isolated algal species (molecularly identified as *C. sorokiniana* and *S. pectinatus*) when *pH* values were adjusted to 7.5 at 25 °C. Hence, under such conditions, we ensure that 98% of TAN (ranging from 10 to 110 $mgN.L^{-1}$) was present as NH_4^+ form (see the relative proportion of NH_3 and NH_4^+ as a function of *pH* at 25 °C³⁸). Under this range of concentrations, no significant difference in the growth rates of *S. pectinatus* or *C. sorokiniana* was measured ($p > 0.05$, ANOVA from ANOCOVA test results for four observations; see Fig. 1(a)). Therefore, the NH_4^+ form at such concentrations, typically found in wastewaters, did not affect the growth rates of both microalgae. Similarly, it was reported that species such as *Chlorella* are very tolerant to high TAN concentrations (max. 140 and 250 $mgN.L^{-1}$ stated respectively in Collos and Harrison³⁵ and Tam and Wong³⁹). However, Przytocka-Jusiak *et al.*⁴⁰ reported that cell division of *C. vulgaris* was inhibited at greater TAN concentrations (>300 $mgN.L^{-1}$). Studies performed on *S. acuminatus* showed that cell growth was inhibited only when NH_4^+ concentrations were higher than 200 $mg.L^{-1}$ (see reference⁴¹). Interestingly, it has been previously reported that algal photosynthesis of *S. obliquus* was inhibited at TAN above 28 $mgN.L^{-1}$ if the culture *pH* exceeded 8.0 (see ref.³²).

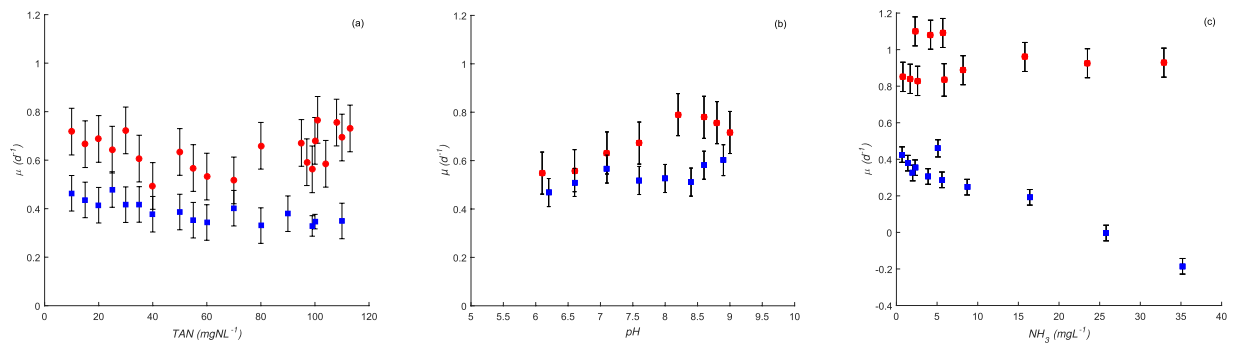


Figure 1. Growth rates from multiple comparisons on growth rate values estimated based on ANOCOVA analyses for *C. sorokiniana* (in red) and *S. pectinatus* (in blue) at different levels of (a) TAN concentrations, (b) pH conditions, (c) NH_3 concentrations.

Because pH can vary during algal growth in ecosystems due to the rapid and large CO_2 consumption of microalgae, this might directly or indirectly affect algal growth rates. The optimal pH of many freshwater algae is about 8 (see ref.⁴²). The growth of many algal species is inhibited in waters at pH greater than 8 (reduction of productivity of *Chaetoceros sp.* and *Chlorella sp.* by 22 % when pH was raised from 8 to 9), while other species can grow well above pH 8 (e.g. *Amphora sp.* and *Ankistrodesmus sp.* at pH 9 and 10, respectively)⁴³. High pH conditions limit the availability of CO_2 while HCO_3^- dominates, and then algae cannot efficiently accumulate carbon and require a high supply of carbonates for maintaining photosynthetic activity⁴² or reducing the affinity to free CO_2 ^{44,45}. During the second set of experiments SE2, the direct effect of pH was tested using pH values ranging from 6 to 9 on algal growth under low initial TAN concentration of about 1 mgN.L^{-1} . As shown in Fig. 1(b), the tested pH conditions had no significant effect on the growth rates measured for both species, *S. pectinatus* and *C. sorokiniana* ($p > 0.05$, ANOVA from ANOCOVA test results for three replicates and three observations). Then, similar to high values of NH_4^+ , the results did not support the hypothesis of a negative effect of high pH values on the growth rates of both studied species when cultured in medium containing 1 mgN.L^{-1} of TAN concentrations. Similarly, Azov and Goldman⁴⁴ suggested that pH did not play a role in the magnitude of inhibition but the degree of dissociation of nontoxic NH_4^+ to toxic NH_3 . In other words, the dissociation of TAN as a function of pH is the main determinant of how much NH_3 is available to inhibit photosynthesis. We suggest that NH_3 concentrations in SE1 and SE2 were likely too low ($< 2 \text{ mg.L}^{-1}$) to exhibit algal growth inhibition. Therefore, the effect of a broader range of NH_3 concentrations was then tested on both species in the third set of experiments.

Evidence of species-dependent ammonia effect. NH_3 is considered the TAN's most toxic form for aquatic organisms⁴⁶. The third set of experiments SE3 was then performed on the same algal isolates (*C. Sorokiniana* and *S. pectinatus*) to test their growth under NH_3 concentrations ranging from 0.56 to 29.42 mgN.L^{-1} . The results for the growth rates of both isolates (represented in Fig. 1(c)) showed that the growth rates of *C. sorokiniana* measured under the different NH_3 concentrations were similar ($p > 0.05$, ANOVA from ANOCOVA test results for three replicates and three observations). However, the growth rates of *S. pectinatus* were significantly different ($p < 0.05$, ANOVA from ANOCOVA test results for three replicates and three observations) with an important reduction in growth rates when NH_3 exceeded 8.7 mg.L^{-1} . Similarly, early works reported that NH_3 at concentrations greater than 15 mgN.L^{-1} and at pH values over 8 inhibited the photosynthesis and growth of *S. obliquus*^{31,44}. The resistance of *C. sorokiniana* to very high NH_3 concentrations (362 mg.L^{-1}) was previously reported⁴⁷, suggesting that species can also adapt their metabolism and becoming more tolerant to high NH_3 environments over time^{31,40}.

In HRAPs initially supplemented with high TAN concentrations, NH_3 toxicity is therefore expected to be associated with elevated pH due to intense photosynthetic activity³¹ and could cause the depletion of microalgae culture or promote replacement with other tolerant species to face the prevailing stress. This feature should be magnified considerably during the summer as the conversion between NH_4^+ and NH_3 is also temperature dependent⁴⁸.

Evidence of facilitation interaction through a modeling approach. A modeling approach was used to identify the growth characteristics of both studied species to predict their dynamics when they are growing together. Based on nutrient dynamics monitored in the HRAP²⁷, we assumed that TAN was the sole limiting substrate driving the algal growth. Moreover, we considered that NH_3 would have a direct inhibitory effect on cell growth, whose fraction is given by the following expression:

$$f(pH, T) = \frac{1}{1 + 10^{pKa(T) - pH}}$$

with $pKa(T) = 0.09018 + \frac{2727.92}{T + 273.15}$ (established within the temperature range of $0 \text{ }^\circ\text{C}$ – $50 \text{ }^\circ\text{C}$ and a pH range of 6.0 to 10.0 (see⁴⁸)).

As a first step, species growth rates were related to external TAN concentrations to calibrate one kinetic model, which could represent satisfactorily most of the data points of the previous test experiments obtained in both SE2

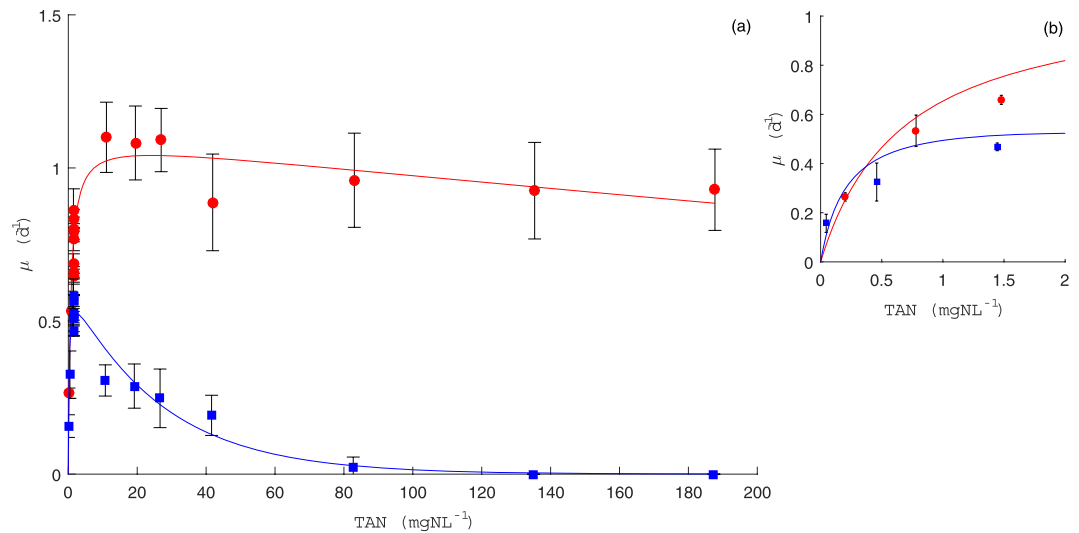


Figure 2. SE2 and SE3 data sets (full points) compared to the proposed kinetic model for *C. sorokiniana* (continuous red line) and *S. pectinatus* (continuous blue line) in (a), with a focus on low TAN concentrations in (b) (Data points are the mean of 3 duplicate measurements of growth rate).

Parameter	<i>C. sorokiniana</i>	<i>S. pectinatus</i>
$\hat{\mu}$ (d ⁻¹)	1.10	0.63
k (mgNL ⁻¹)	0.68	0.22
k_i (mgNH ₃ -N.L ⁻¹)	79.82	2.25
$\frac{\hat{\mu}}{k}$	1.62	2.85
J (least squares criterion)	0.08	0.04

Table 1. Calibration results on SE2 and SE3 growth data obtained in batch cultures.

and SE3. The proposed model was inspired from Aiba-Edward's model⁴⁹ describing the substrate inhibition at high concentrations and consisting of a modified version of the Monod equation⁵⁰, but here it has a slightly different mathematical expression as explained below. While Monod kinetics assumed that only one nutrient limits the growth of cells, the model we propose here includes that a by-product of this limiting nutrient (free ammonia nitrogen NH₃-N) negatively affects cells growth as given by the following expression:

$$\mu(TAN, pH, T) = \hat{\mu} \frac{TAN}{k + TAN} e^{-\frac{TAN f(pH, T)}{k_i}} \quad (1)$$

where $\hat{\mu}$ is the maximum growth rate (d⁻¹), k is the affinity to substrate (mg.L⁻¹), k_i is the inhibition constant of NH₃-N (mg.L⁻¹) and $f(pH, T)$ is defined above. This growth function provided a good fit to experimental data describing the growth kinetics of the two species (see Fig. 2). The identified kinetic parameters are given in Table 1. From the fit of this kinetic model to data, the species *S. pectinatus* showed a strong affinity for nitrogen with a greater $\frac{\hat{\mu}}{k}$ ratio than that obtained for *C. sorokiniana* (see also the comparison of the two species kinetics with a particular focus on low TAN concentrations in Fig. 2(b)). In contrast, this latter species has a maximum growth rate (1.10 d⁻¹) much higher than that of *S. pectinatus* (0.63 d⁻¹). Consequently, *C. sorokiniana* would grow well at high TAN concentrations and would also tolerate high NH₃ concentrations as reported by its highest inhibition constant ($k_i = 79.82$ mgNH₃-N.L⁻¹), while *S. pectinatus* would grow best at low TAN concentrations but would show a much faster decline in growth because of its high sensitivity to NH₃ toxicity represented by a low k_i (2.25 mgNH₃-N.L⁻¹). Our results are in accordance with older chemostat experiments comparing *S. acutus* and *C. minutissima* under P-limited growth⁵¹.

The ecological succession of species presenting Monod- and Haldane⁵² kind growth functions have already been shown theoretically⁵³ but not yet experimentally. The Monod and Haldane kinetics were fitted to our data (results not shown). Their graphs closely resemble those given by (1), but with a higher least squares criterion J .

Knowing the growth performances of each species in the laboratory (Fig. 3(a)), we proposed a predictive model to explore how the assemblage of the two species might react under a fixed pH (8.6) and temperature (25 °C) in continuous culture to check if the hypothesis of ecological facilitation is verified. We used the initial conditions of substrate and biomass and the operational conditions (dilution rate and input substrate concentration) encountered in the previous study on HRAPs²⁷. The results of our simulations are summarized in Fig. 3. These simulations revealed that *S. pectinatus* is unable to grow and is washed out because of the NH₃ toxicity when cultivated

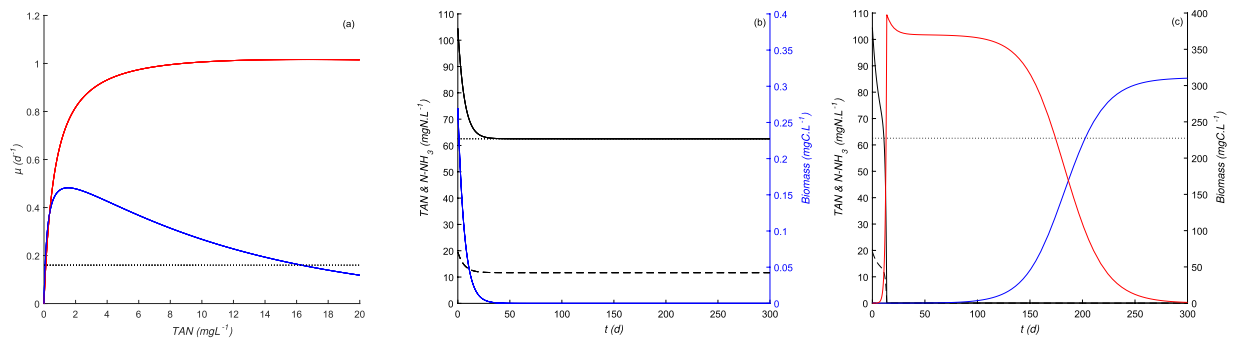


Figure 3. Simulation results obtained under a continuous supply with a high TAN concentration (dotted line in (b,c)) at a fixed dilution rate (dotted line in (a)). (a) growth functions previously identified for *C. Sorokiniana* (in solid red line) and *S. pectinatus* (in solid blue line), (b) dynamics when *S. pectinatus* is cultivated alone, (c) dynamics when *S. pectinatus* and *C. Sorokiniana* are cultivated together. In (b,c), the biomass variations over time are presented in blue for *Scenedesmus sp.* and in red for *Chlorella sp.* while the substrate variations are in solid black lines for TAN and in black dashed lines for NH_3 .

alone under high TAN and pH conditions (see Fig. 3(b)). However, when both microalgae are introduced together under these latter conditions, *C. sorokiniana* grows rapidly first while the growth of *S. pectinatus* is inhibited because of high NH_3 . The rapid consumption of the nitrogen resource by *C. sorokiniana* induces low NH_3 and less nitrogen availability, favoring the growth of the competitive *S. pectinatus* but not *C. sorokiniana* (see Fig. 3(c)). Therefore, the ecological facilitation between *C. sorokiniana* and *S. pectinatus* would be induced by NH_3 toxicity and would explain their succession. These results also support the empirical evidence in plant communities that the balance between facilitation and competition can shift along an environmental gradient, with facilitation being successively more important in harsh environments²⁰.

Importance of the initial populations densities on the degree of facilitation in simulated HRAP.

Using the mathematical approach, we explored the influence of the initial densities of the studied species on some indicators of facilitation degree, which might be useful to further explore the optimization strategies for algal biomass production under high levels of ammonia stress in HRAP. There are different advantages to having a *Scenedesmus* dominance in an HRAP supplemented with wastewaters, as this species possesses a high affinity to nitrogen, is strongly resilient to predators⁵⁴, and its biomass can be easily harvested⁵⁵ and used for different purposes (e.g. lipid production⁵⁶). For these reasons, we proposed to study theoretically some proxies of the facilitation efficiency such as resilience and succession times to provide information on the time required for the development of *S. pectinatus* in the HRAP under the previously stated operating conditions.

We defined the resilience time as the duration for *S. pectinatus* to reach its initial biomass value under the presence of the toxic NH_3 concentrations. Moreover, because the succession of the two microalgae is required for maintaining *S. pectinatus* under high nutrient toxic levels, we also defined the succession time as the time for which the two species reach twice the same density level owing to the predominance of *S. pectinatus*. We plotted the iso-values of the resilience and succession times in the (A_1, A_2) plane, where A_1, A_2 are the initial densities of each species (see Fig. 4). These diagrams allow to see easily for which pairs of initial densities (A_1, A_2) one may expect low or high resilience or succession time (the shortest time is in blue, and the longest one is red). The diagram in Fig. 4(a) shows that the resilience time is more affected by the initial biomass concentrations of *C. sorokiniana* than that of *S. pectinatus*. This contrasts with the succession time (in Fig. 4(b)) which is more sensitive to the initial concentrations of *S. pectinatus*, especially when *C. sorokiniana* is initiated at concentrations values higher than 1 mg C L^{-1} . Such simulation would be of interest in further control of the diversity within an HRAP supplemented with wastewaters, especially for managing the periods of dysfunction (e.g. sudden algal crash, variations in wastewaters inflow). For example, it could be suggested to increase the initial concentration of *C. sorokiniana* (at a concentration higher than 6 mg C L^{-1}) through bioaugmentation to ensure a rapid reduction of NH_3 toxicity and rapid development of *S. pectinatus* in a minimum of 25 days. On the other hand, the time needed for *S. pectinatus* predominance over *C. sorokiniana* will depend on the initial concentration of *S. pectinatus* and the higher the *S. pectinatus*'s initial concentration would be ($>12 \text{ mg C L}^{-1}$) the faster the succession would occur (minimum of 80 days). Consequently, our theoretical results depicted with iso-value diagrams showed that the algal resilience and succession times within an intensive algal ecosystem are strongly dependent on the initial populations' densities that may be used to control algal production processes in HRAPs.

Validation of the ecological facilitation in real HRAP. The dynamics of the biomass of *Chlorella sp.* and *Scenedesmus sp.* and the TAN concentrations measured in HRAP operating from 28 April 2015 to 8 September 2015 in Northern France²⁷ were compared to model simulations (see Fig. 5) using the growth functions parameters of *C. sorokiniana* and *S. pectinatus* represented in Table 1. We made few changes to the initial model by adding mortality terms and considering different yields parameters values from those determined experimentally (all regarded as unknown constants) thus, still keeping the set of equations as simple as possible. The mortality terms were added to take into account the grazing effect on each algal species in an indirect way given the presence of predators in the HRAP. Changes in yield coefficients was requested knowing that heterotrophic bacteria were

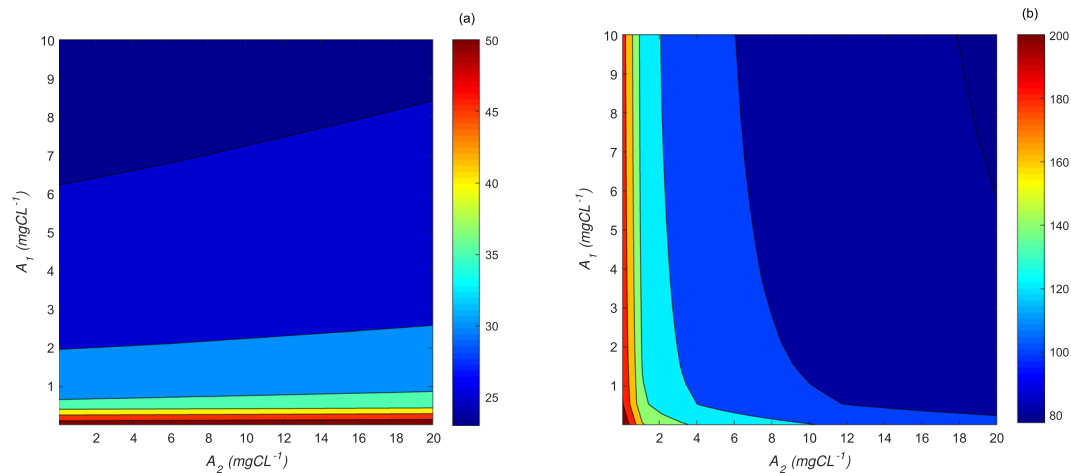


Figure 4. Isovalue diagrams: resilience time (a) and succession time (b) (in days) depending on the initial biomass densities of *C. sorokiniana* (A_1) and *S. pectinatus* (A_2) (in mgC.L⁻¹) under a continuous supply of a high nitrogen concentration.

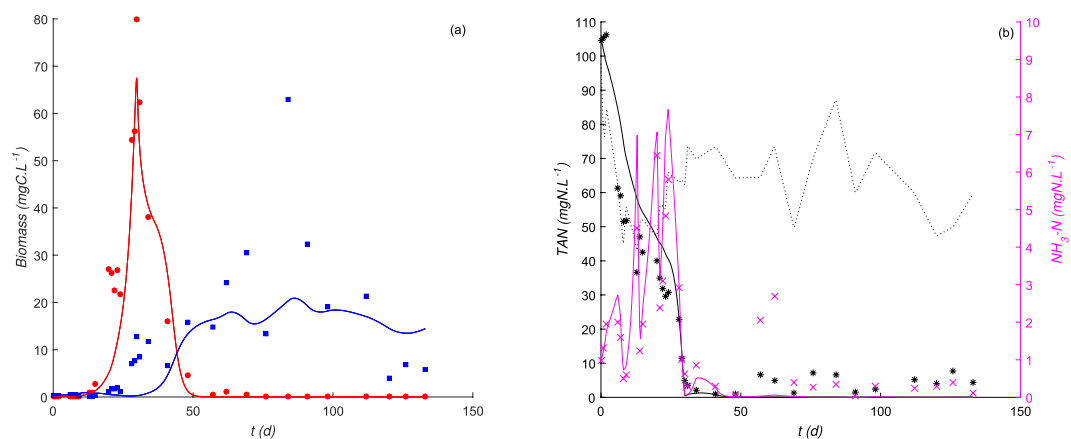


Figure 5. HRAP data points compared to the model prediction (in continuous lines) under a continuous supply of wastewater containing fluctuating concentrations of TAN (dotted black line). (a) Biomass variations over time of *Chlorella sp.* (in red) & *Scenedesmus sp.* (in blue), (b) substrate variations over time of TAN (in black) & NH₃ (in magenta).

Parameter	<i>C. sorokiniana</i>	<i>S. pectinatus</i>
y^* (gC/gN)	2.81	0.30
m^* (d ⁻¹)	0.58	0.02
J (least squares criterion)	96.72	

Table 2. Calibration results on HRAP data.

also growing in the pond and consuming nitrogen. The estimated parameters of yield and mortality coefficients obtained from the comparison of the model dynamics with data from HRAP are presented in Table 2. Assuming that higher predation pressure corresponds to a higher mortality coefficient, our results suggest that *Chlorella sp.* was likely more sensitive to grazing than *Scenedesmus sp.* known to produce a grazer-morphological defense according to a previous study⁵⁴. However, the washout of *Chlorella sp.* at the system steady-state is probably not due to high pressure by a high mortality coefficient but rather to competition with *Scenedesmus sp.* when the environment becomes depleted of the nitrogen resource, as demonstrated through the previous simulation results in Fig. 3(c).

We noted that the estimated yields coefficients in laboratory chemostat experiments after three days at steady-state (i. e. 5.9 ± 0.7 gC/gN and 5.0 ± 0.6 gC/gN for *C. sorokiniana* and *S. pectinatus*, respectively) were higher than those identified in the HRAP (see Table 2), which may be explained by the presence of denitrifying bacteria producing N₂ subsequently lost through degassings²⁷.

In the HRAP, the first bloom of *Chlorella* sp. happened at high concentrations of NH_3 and has been replaced later by the bloom of *Scenedesmus* sp. (data in Fig. 5(a)). The distribution of these species was consistent with our experimental and modeling results on the species *C. sorokiniana* and *S. pectinatus* (see Fig. 3). This validates the importance of facilitation during the biological colonization of the HRAP under toxic levels of NH_3 . These results confirmed our initial hypothesis that the colonization of hypertrophic ecosystems by the stress-tolerant *Chlorella* sp. is a prerequisite for the development of the sensitive *Scenedesmus* sp. to NH_3 toxicity. *Chlorella* is usually considered as an invasive phytoplankton or pioneer species because it maintains fast growth rates and assimilates resources with short generation times, and can dominate over slower-growing species^{57,58}. In contrast, *Scenedesmus* is considered an affinity specialist⁵¹, and it can dominate in HRAPs over *Chlorella* and colonize the HRAP²⁷ at low and nontoxic nutrient levels. Therefore, based on the model confrontation to real data in HRAP, pioneer organisms (here *Chlorella*) can modify their chemical environment by reducing ammonia toxicity, which can increase the fitness of the growth of sensitive and specialist organisms (here *Scenedesmus*).

Our study sheds a light on an ecological interaction within aquatic microbial communities that is rarely discussed in the literature, although it may explain ecological successions that occur without any visible external variations of growth conditions or mortality. Similarly to various types for macro-organisms²¹, the ability of aquatic microorganisms to drastically modify their immediate environment would impact the growth of neighbors. Because microalgae can change their light environment when growing (i. e. light attenuation by algal biomass), the growth of photoinhibited algal species can be facilitated by the biomass of other algal species less sensitive to photoinhibition²⁶. In a similar way, under toxic metal stress, it has been suggested that the growth of Cd-sensitive microalgal species may be promoted by Cd-tolerant microalgal species reducing Cd in the media to low levels⁵⁹. Therefore facilitation within the aquatic microbial communities through the reduction of inhibiting factors is likely to be a widespread interaction applied for a large range of environmental stress.

Materials and Methods

HRAP experiment. The pre-existing data used in this study were obtained in HRAP of 1.9 m³ working volume, continuously fed by pre-treated wastewaters (after screening and removing grit, sand, and grease) with a constant retention time of 6 days (see²⁷). Algal blooms occurred naturally in the open pond without any algal inoculation. The period covered by this study was from 28 April 2015 to 8 September 2015. For the present study, we used the data obtained through analytical monitoring that was performed on the influent wastewater and on samples taken from the HRAP. They included water temperature, chemical analyses (TAN and pH), and the algal biomass of the two dominant algal species (*Chlorella* sp. and *Scenedesmus* sp., which were identified by microscopy) estimated using cell count from flow cytometry and converted into carbon units.

Microalgae strains, cultivation conditions, and laboratory experiments. One Strain of freshwater microalgae *Chlorella* sp. and *Scenedesmus* sp. was isolated from the HRAP samples taken in October 2015. Individual strains were isolated in Z8 media⁶⁰. The Z8 media was modified to Z8NH₄ by replacing all nitrogen forms with ammonium salt (NH₄Cl) as the sole source of nitrogen in the growth medium and by adding the HEPES buffer at 20 mM. The two species were maintained and cultivated under continuous light (100 $\mu Em^{-2}s^{-1}$) and temperature (25 °C). We performed three sets of experiments (SE1, SE2 and SE3) in batch reactors with a working volume of 40 mL. Each set was preceded by a pre-incubation phase in which the two species are pre-adapted to the fixed cultivation conditions in each set of experiments and providing sufficient fresh volumes for inoculations. The pre-incubations were performed either in continuous mode (in 2 L photobioreactors stirred at 300 rpm, one-sided illuminated at 130 $\mu Em^{-2}s^{-1}$, before SE1) or in batch mode (in a shaken flask at 150 rpm of 200 mL, before SE2 and SE3). All batch experiments (in pre-incubation or in the three-test sets) were performed in laboratory incubators under a temperature set at 25 °C ± 2 °C, an orbital agitation at 150 rpm speed and an incident light intensity set at 50 $\mu Em^{-2}s^{-1}$ in SE2 and SE3.

The first pre-incubation in continuous photobioreactors were performed to determine the yield constants and provide sufficient fresh volumes for later inoculation in batch culture. Thus, each strain was growing for about 15 days until the biomass stabilization, under a constant temperature of 25 °C and a continuous supply of sterilized medium (C:N:P ratio at about 1:34:1) at a fixed pH value of 7.5 and a fixed dilution rate (0.25 d⁻¹). After that, the growth of the two species was assessed in batch cultures (as described above) under different initial TAN concentrations ranging from 10 to 110 mg.L⁻¹ keeping constant the concentrations of all other medium components. The pH value was maintained at 7.5 in all batch reactors of SE1.

In the second set of experiments SE2, prior to the experiment, the two species were pre-incubated in batch cultures for about 6 days in a sterilized medium of modified Z8NH₄ with a C:N:P ratio at about 88:2:1 and a pH set at 7.5. Then, SE2 experiments were performed (as described above) under different pH conditions initially adjusted to 6.0, 6.5, 7.0, 7.5, 8.0, 8.4, 8.7, and 9.0 with NaOH or HCl while using a similar initial concentration of NH₄Cl of 2 mg.L⁻¹ that was supposed to be nontoxic for both microalgae strains.

Prior SE3, the 6-days pre-incubation of two species was performed in a sterilized medium of modified Z8NH₄ with a C:N:P ratio at about 88:8:1 and a fixed pH value initially set at 8.6 (corresponding to the average value of pH measured in HRAP). Finally, in SE3, the growth of the two species was assessed in batch cultures under a large range of initial NH₄Cl from 1.2 to 187.7 mg.L⁻¹ keeping the pH at 8.6.

DNA isolation, PCR, and sequencing. Genomic DNA was extracted from a 10 mL sample filtered onto a 0.2 μm membrane (PALL Supor 200 PES), using the standard phenol/chloroform method⁶¹. The 18S and ITS rDNA were amplified in PCR reactions using the Pfu polymerase (Promega) with the primers EAF3 (5'-TCGACAATCTGGTTGATCCTGCCAG-3') and ITS055R (5'-CTCCTTGGTCCGTGTTTCAAGACGGG-3')⁶². The PCR products were purified using the QIAquick Gel Extraction Kit (Qiagen) and sequenced

using two primers (V4 Forward: 5'-AATTCCAGCTCCAATAGCGTATAT-3' and ITS Forward: 5'-CCTTTGTACACACCGCCCGTCG-3') to target specifically the variable V4 region of the 18S rDNA and the ITS region. Sanger sequencing was performed at Eurofins Genomics (GATC services).

Sample analyses. The *pH* in each culture solution was determined daily (*pH* meter Symphony SP70P, VWR). For algal biomass estimation, samples were shaken to bring all the cells into suspension and subsamples were daily taken to measure absorbance. In *SE1*, the growth of algae was measured using optical density *OD* of the culture with a microplate reader (FLUOSTAR, BMG Labtech) at 650 nm. In *SE2* and *SE3*, cell mass was measured by fluorescence (EX 450 nm, EM 680 nm) and *OD* at 650 nm, 730 nm, and 680 nm using a microplate reader (CHAMELEON, Hidex). Two different readers have been used due to a technical problem in CHAMELEON after the *SE1* period.

In *SE2* and *SE3*, subsamples were collected at the beginning and at the end of each experiment, for nutrient and biomass analysis. Samples were then filtered using (i) 0.2 μm Sartorius filters for measuring nutrients in filtrates and (ii) pre-combusted AE filters for measuring carbon biomass onto filters. Ammonia nitrogen was measured with a spectrophotometric test kit (SpectroQuant, Merck Millipore) and orthophosphate phosphorus according to an optimized molybdenum blue method⁶³. After drying the filters (24 h, 60 °C), the particulate organic carbon representing mainly algal carbon biomass was analysed using an ANCA mass spectrometer (Europa Scientific).

Data analysis. We performed the covariance analysis using the “aoctool” function of Matlab to compare significant differences in growth rates μ of algae after 48 h exposure at each tested condition. The technique required the grouped data of logarithm of the biomass $\ln(x)$ measured at time t (during the time period 0 to 48 h) for all tested condition. We modelled $\ln(x)$ as a linear function of t to determine whether the slope of the line, which represents an estimate of μ , varies among groups. Based on the model fit of the separate-lines model, the stats output structure from “aoctool” served as input to the multi-compare test “multcompare” function of Matlab, which allows for testing either slopes or intercepts.

Modeling procedures. The first identifications of the growth function parameters for the two species were performed by fitting the proposed kinetic model (1) to the assessed values of specific growth rate data obtained in *SE2* and *SE3* for which cultivation conditions are either identical or different but would not be disruptive of the growth rates except for the initial *TAN* concentration. The optimal growth parameters were calibrated by the “fmincon” function of Matlab optimization toolbox used in minimizing a mean square criterion $J = \sum_{i=1}^n (\mu_{i_{exp}} - \mu_{i_{sim}})^2$, where $\mu_{i_{exp}}$ and $\mu_{i_{sim}}$ are the normalized experimentally estimated and model generated values of growth rates at the i^{th} experimental condition, and n is the total number of estimated growth rates corresponding to the total number of tested conditions *TAN* concentrations in *SE2* and *SE3*.

Secondly, we used the identified growth functions on (1) to simulate the following system (2) in order to explore the species dynamics under a fixed *pH* (8.6) and temperature (25 °C) in a homogeneous continuous reactor.

$$\begin{cases} \dot{A}_1 &= (\mu_1(N) - D)A_1 \\ \dot{A}_2 &= (\mu_2(N) - D)A_2 \\ \dot{N} &= -\frac{1}{y_1}\mu_1(N)A_1 - \frac{1}{y_2}\mu_2(N)A_2 + D(N_{in} - N) \end{cases} \quad (2)$$

This set of equations gives the variations over the time of both algal biomass of *C. sorokiniana* and *S. pectinatus* (in mgC.L^{-1}) and substrate concentrations ($\text{TAN} = \text{NH}_3 + \text{NH}_4^+$) (in mgN.L^{-1}), denoted $A_1(t)$, $A_2(t)$ and $N(t)$, respectively. The growth functions $\mu_1(N)$ and $\mu_2(N)$ depend only on *TAN* (when $T = 25$ °C and *pH* = 8.6, according to (1) and the parameters presented in Table 2), as the sole source of nitrogen supplied continuously at the fixed dilution rate $D = 0.16 \text{ d}^{-1}$ and the constant concentration $N_{in} = 62.54 \text{ mgN.L}^{-1}$ of wastewater encountered in the studied *HRAP*. The yield coefficients were taken equal to $y_1 = 5.93 \text{ gC/gN}$ and $y_2 = 4.98 \text{ gC/gN}$ for *C. sorokiniana* and *S. pectinatus*, respectively. These values were theoretically calculated from continuous photobioreactors experiments performed at pre-incubation for *SE1* and given by $y_i = \frac{A_i^*}{N_{in} - N_i^*}$, where A_i^* and N_i^* are respectively the algal biomass and nitrogen concentrations at steady-state). The system (2) was solved using “ode23t” differential equation solver using the following initial conditions of substrate and biomass: $N_0 = 104.50 \text{ mgN.L}^{-1}$, $A_{10} = 0.0123 \text{ mgC.L}^{-1}$ and $A_{20} = 0.2698 \text{ mgC.L}^{-1}$.

Under the same conditions as mentioned above, we theoretically studied the algal resilience and succession times as proxies of the facilitation efficiency for different initial biomass concentrations (in mgC.L^{-1}) ranging between [0.0123, 10] and [0.05, 20] for *C. sorokiniana* and *S. pectinatus*, respectively. The iso-value diagrams were obtained using the “contourf” plot of Matlab.

Third, we validated the hypothesis of ecological facilitation on real dynamics in *HRAP*. We used the whole dynamics simulated over the time from the given initial condition until the system was at a quasi steady-state and we compared data to the following model Eq. (3) including terms of mortality m_1^* and m_2^* on A_1 and A_2 , respectively:

$$\begin{cases} \dot{A}_1 &= (\mu_1(N, pH, T) - D - m_1^*)A_1 \\ \dot{A}_2 &= (\mu_2(N, pH, T) - D - m_2^*)A_2 \\ \dot{N} &= -\frac{1}{y_1^*}\mu_1(N, pH, T)A_1 - \frac{1}{y_2^*}\mu_2(N, pH, T)A_2 + D(N_{in} - N) \end{cases} \quad (3)$$

In this new set of Eq. (3), we considered the variations over the time of N_m , pH , and T implemented into the model with interpolations performed between the real data points measured over time within the HRAP. We identified the unknown parameters (m_1^* , m_2^* , y_1^* , and y_2^*) of the dynamic model using “fmincon” function of Matlab optimization toolbox. The optimal parameters assuring the best fit to data were constrained to be positive and defined in predefined intervals of boundary values after 100 consecutive estimations. Mortality constants were estimated within the interval [0, 1] (d^{-1}), while yields coefficients were supposed to be ranged between *i*) minimal values theoretically calculated during the period of the dominance of each species in the HRAP (i. e. 1.3 ± 0.1 gC/gN and 0.5 ± 0.2 gC/gN for *Chlorella sp.* and *Scenedesmus sp.*, respectively) and *ii*) maximal values identified in our laboratory chemostat experiments after three days at steady-state (i. e. 5.93 ± 0.66 gC/gN and 4.98 ± 0.58 gC/gN for *C. sorokiniana* and *S. pectinatus*, respectively). The mean squared error was used as the criterion function for the model parameters estimation and was calculated as the square root of the variance of the observations (of A_1 , A_2 and N) and divided by the number of measurements.

Received: 1 July 2019; Accepted: 14 October 2019;

Published online: 05 November 2019

References

- Kilham, P. & Hecky, R. E. Comparative ecology of marine and freshwater phytoplankton 1. *Limnol. Oceanogr.* **33**, 776–795 (1988).
- Diamant, Q. Hierarchical control of phytoplankton succession by physical factors. *Mar. Ecol. Prog. Ser.* **19**, 211–222 (1984).
- Barbiero, R. P., James, W. F. & Barko, J. W. The effects of disturbance events on phytoplankton community structure in a small temperate reservoir. *Freshw. Biol.* **42**, 503–512 (1999).
- Grover, J. P. & Chrzanowski, T. H. Seasonal dynamics of phytoplankton in two warm temperate reservoirs: association of taxonomic composition with temperature. *J. Plankton Res.* **28**, 1–17 (2006).
- Lewandowska, A. & Sommer, U. Climate change and the spring bloom: a mesocosm study on the influence of light and temperature on phytoplankton and mesozooplankton. *Mar. Ecol. Prog. Ser.* **405**, 101–111 (2010).
- Deng, J. *et al.* Effects of nutrients, temperature and their interactions on spring phytoplankton community succession in lake taihu, china. *PLoS One* **9**, e113960 (2014).
- Gaedeke, A. & Sommer, U. The influence of the frequency of periodic disturbances on the maintenance of phytoplankton diversity. *Oecologia* **71**, 25–28 (1986).
- Nöges, T., Nöges, P. & Laugaste, R. Water level as the mediator between climate change and phytoplankton composition in a large shallow temperate lake. *Hydrobiologia* **506**, 257–263 (2003).
- Robinson, J. F. & Dickerson, J. E. Does invasion sequence affect community structure? *Ecology* **68**, 587–595 (1987).
- Havens, K. E. Experimental perturbation of a freshwater plankton community: a test of hypotheses regarding the effects of stress. *Oikos* 147–153 (1994).
- Leibold, M. A. Biodiversity and nutrient enrichment in pond plankton communities. *Evol. Ecol. Res.* **1**, 73–95 (1999).
- Aneesh, C. N., Haridas, A. & Manilal, V. B. Role of nutrients input pattern on the growth dynamics of common freshwater microalgal community. *Am. J. Plant Sci.* **6**, 2481 (2015).
- Tilman, D. *Resource competition and community structure* (Princeton university press, 1982).
- Porter, K. G. The plant-animal interface in freshwater ecosystems: microscopic grazers feed differentially on planktonic algae and can influence their community structure and succession in ways that are analogous to the effects of herbivores on terrestrial plant communities. *Am. Sci.* **65**, 159–170 (1977).
- Margalef, R. Life-forms of phytoplankton as survival alternatives in an unstable environment. *Ocean. Acta* **1** (1978).
- Smayda, T. Phytoplankton species succession. *The Physiol. Ecol. Phytoplankton.* 493–570 (1980).
- Anneville, O. *et al.* Temporal mapping of phytoplankton assemblages in lake geneva: annual and interannual changes in their patterns of succession. *Limnol. Oceanogr.* **47**, 1355–1366 (2002).
- Reynolds, C. S. *Vegetation processes in the pelagic: a model for ecosystem theory*, vol. 9 (Ecology Institute Oldendorf, 1997).
- Johnson, R. E., Tuchman, N. C. & Peterson, C. G. Changes in the vertical microdistribution of diatoms within a developing periphyton mat. *J. North Am. Benthol. Soc.* **16**, 503–519 (1997).
- Bruno, J. F., Stachowicz, J. J. & Bertness, M. D. Inclusion of facilitation into ecological theory. *Trends Ecol. & Evol.* **18**, 119–125 (2003).
- Stachowicz, J. J. Mutualism, facilitation, and the structure of ecological communities: positive interactions play a critical, but underappreciated, role in ecological communities by reducing physical or biotic stresses in existing habitats and by creating new habitats on which many species depend. *Bioscience* **51**, 235–246 (2001).
- Connell, J. H. & Slatyer, R. O. Mechanisms of succession in natural communities and their role in community stability and organization. *The Am. Nat.* **111**, 1119–1144 (1977).
- Stevenson, R. J. Effects of current and conditions simulating autogenically changing microhabitats on benthic diatom immigration. *Ecology* **64**, 1514–1524 (1983).
- Roemer, S. C., Hoagland, K. D. & Rosowski, J. R. Development of a freshwater periphyton community as influenced by diatom mucilages. *Can. J. Bot.* **62**, 1799–1813 (1984).
- Hansen, P. J. Effect of high pH on the growth and survival of marine phytoplankton: implications for species succession. *Aquatic Microb. Ecol.* **28**, 279–288 (2002).
- Gerla, D. J., Mooij, W. M. & Huisman, J. Photoinhibition and the assembly of light-limited phytoplankton communities. *Oikos* **120**, 359–368 (2011).
- Galès, A. *et al.* Importance of ecological interactions during wastewater treatment using high rate algal ponds under different temperate climates. *Algal Res.* **40**, 101508 (2019).
- Canovas, S. *et al.* Seasonal development of phytoplankton and zooplankton in a high-rate algal pond. *Water Sci. Technol.* **33**, 199 (1996).
- Cho, D.-H. *et al.* Microalgal diversity fosters stable biomass productivity in open ponds treating wastewater. *Sci. Reports* **7**, 1979 (2017).
- Schlüter, M., Groeneweg, J. & Soeder, C. J. Impact of rotifer grazing on population dynamics of green microalgae in high-rate ponds. *Water Res.* **21**, 1293–1297 (1987).
- Abeliovich, A. & Azov, Y. Toxicity of ammonia to algae in sewage oxidation ponds. *Appl. Environ. Microbiol.* **31**, 801–806 (1976).
- Goldman, J. C., Azov, Y., Riley, C. B. & Dennett, M. R. The effect of pH in intensive microalgal cultures. i. biomass regulation. *J. Exp. Mar. Biol. Ecol.* **57**, 1–13 (1982).
- Källqvist, T. & Svenson, A. Assessment of ammonia toxicity in tests with the microalga, *nephroselmis pyriformis*, chlorophyta. *Water Res.* **37**, 477–484 (2003).
- Wang, J. *et al.* Ammonium nitrogen tolerant chlorella strain screening and its damaging effects on photosynthesis. *Front. Microbiol.* **9** (2018).

35. Collos, Y. & Harrison, P. J. Acclimation and toxicity of high ammonium concentrations to unicellular algae. *Mar. Pollut. Bull.* **80**, 8–23 (2014).
36. Natarajan, K. Toxicity of ammonia to marine diatoms. *J. Water Pollut. Control. Fed.* R184–R190 (1970).
37. Admiraal, W. Tolerance of estuarine benthic diatoms to high concentrations of ammonia, nitrite ion, nitrate ion and orthophosphate. *Mar. Biol.* **43**, 307–315 (1977).
38. König, A., Pearson, H. & Silva, S. A. Ammonia toxicity to algal growth in waste stabilization ponds. *Water Sci. Technol.* **19**, 115–122 (1987).
39. Tam, N. & Wong, Y. Effect of ammonia concentrations on growth of *Chlorella vulgaris* and nitrogen removal from media. *Bioresour. Technol.* **57**, 45–50 (1996).
40. Przytowska-Jusiak, M., Młynarczyk, A., Kulesza, M. & Mycielski, R. Properties of *Chlorella vulgaris* strain adapted to high concentration of ammonium nitrogen. *Acta Microbiol. Polonica* **26**, 185–197 (1977).
41. Park, J., Jin, H.-F., Lim, B.-R., Park, K.-Y. & Lee, K. Ammonia removal from anaerobic digestion effluent of livestock waste using green alga *Scenedesmus* sp. *Bioresour. Technol.* **101**, 8649–8657 (2010).
42. Kong, Q.-X., Li, L., Martinez, B., Chen, P. & Ruan, R. Culture of microalgae *Chlamydomonas reinhardtii* in wastewater for biomass feedstock production. *Appl. Biochem. Biotechnol.* **160**, 9 (2010).
43. Weissman, J. C., Goebel, R. P. & Benemann, J. R. Photobioreactor design: mixing, carbon utilization, and oxygen accumulation. *Biotechnol. Bioeng.* **31**, 336–344 (1988).
44. Azov, Y. & Goldman, J. C. Free ammonia inhibition of algal photosynthesis in intensive cultures. *Appl. Environ. Microbiol.* **43**, 735–739 (1982).
45. Rotatore, C. & Colman, B. The active uptake of carbon dioxide by the unicellular green algae *Chlorella saccharophila* and *C. ellipsoidea*. *Plant, Cell & Environ.* **14**, 371–375 (1991).
46. Haywood, G. P. Ammonia toxicity in teleost fishes: a review. *Can. Tech. Rep. Fish. Aquat. Sci.* **1177**, 1–35 (1983).
47. Ogbonna, J. C., Yoshizawa, H. & Tanaka, H. Treatment of high strength organic wastewater by a mixed culture of photosynthetic microorganisms. *J. Appl. Phycol.* **12**, 277–284 (2000).
48. Emerson, K., Russo, R. C., Lund, R. E. & Thurston, R. V. Aqueous ammonia equilibrium calculations: effect of pH and temperature. *J. Fish. Board Can.* **32**, 2379–2383 (1975).
49. Edwards, V. H. The influence of high substrate concentrations on microbial kinetics. *Biotechnol. Bioeng.* **12**, 679–712 (1970).
50. Monod, J. *Recherches sur la croissance des cultures bactériennes*. Ph.D. thesis (1942).
51. Sommer, U. Comparison between steady state and non-steady state competition: experiments with natural phytoplankton. *Limnol. Oceanogr.* **30**, 335–346 (1985).
52. Andrews, J. F. A mathematical model for the continuous culture of microorganisms utilizing inhibitory substrates. *Biotechnol. Bioeng.* **10**, 707–723 (1968).
53. Rapaport, A. & Harmand, J. Biological control of the chemostat with nonmonotonic response and different removal rates. *Math. Biosci. Eng.* **5**, 539–547 (2008).
54. Mayeli, S., Nandini, S. & Sarma, S. The efficacy of *Scenedesmus* morphology as a defense mechanism against grazing by selected species of rotifers and cladocerans. *Aquatic Ecol.* **38**, 515–524 (2005).
55. Grima, E. M., Belarbi, E.-H., Fernández, F. A., Medina, A. R. & Chisti, Y. Recovery of microalgal biomass and metabolites: process options and economics. *Biotechnol. Adv.* **20**, 491–515 (2003).
56. Ahmed, A., Jyothi, N. & Ramesh, A. Improved ammonium removal from industrial wastewater through systematic adaptation of wild type *Chlorella pyrenoidosa*. *Water Sci. Technol.* **75**, 182–188 (2016).
57. Elliott, J., Reynolds, C. & Irish, A. An investigation of dominance in phytoplankton using the protech model. *Freshw. Biol.* **46**, 99–108 (2001).
58. Reynolds, C. S. Environmental requirements and habitat preferences of phytoplankton: chance and certainty in species selection. *Bot. Mar.* **55**, 1–17 (2012).
59. Li, S.-P. *et al.* Effects of species richness on cadmium removal efficiencies of algal microcosms. *J. Appl. Ecol.* **49**, 261–267 (2012).
60. Kotai, J. Instructions for preparation of modified nutrient solution z8 for algae. *Nor. Inst. for Water Res. Oslo* **11**, 5 (1972).
61. Sambrook, J. *et al.* *Molecular cloning: a laboratory manual*. Ed. 2 (Cold Spring Harbour Laboratory Press, 1989).
62. Pröschold, T., Marin, B., Schlösser, U. G. & Melkonian, M. Molecular phylogeny and taxonomic revision of *Chlamydomonas* (Chlorophyta). i. emendation of *Chlamydomonas ehrenbergii* and *Chloromonas gobi*, and description of *Oogamochlamys* gen. nov. and *lobochlamys* gen. nov. *Protist* **152**, 265–300 (2001).
63. Aminot, A. & Kérouel, R. *Hydrologie des écosystèmes marins: paramètres et analyses* (Editions Quae, 2004).

Acknowledgements

We thank Elodie Lanouguère for microalgae isolation and cultivation, Ariane Atteia for identifying the microalgal strains, Martine Fortune for ammonia analyses, Patrick Raimbault for carbon content analyses, and Christine Felix for giving helping hand to experiments monitoring. We would also like to thank Bénédicte Fontez for assistance with statistical analyses, and Jérôme Harmand for fruitful comments and discussions during the MODEMIC research school on resource-consumer models (21–25 September 2015). This study benefited from the HRAP demonstrators developed and operated by SAUR. This work was supported by the ADEME French Agency and the LabEx NUMEV incorporated into the I-Site MUSE funded by the French Research Agency (ANR) that have both funded the PhD grant of the first author. This study was also supported by the PHYCOVER project, which was funded by the French National Agency for Research (ANR-14-CE04-0011).

Author contributions

A.R., E.L.F. and E.F. participated actively in conceiving the experiments, coordinated the research work, and critically revised the manuscript. E.K. designed and conducted laboratory experiments, analyzed data, performed mathematical simulations, and wrote the manuscript.

Competing interests

The authors declare no competing interests.

Additional information

Correspondence and requests for materials should be addressed to E.F.

Reprints and permissions information is available at www.nature.com/reprints.

Publisher's note Springer Nature remains neutral with regard to jurisdictional claims in published maps and institutional affiliations.



Open Access This article is licensed under a Creative Commons Attribution 4.0 International License, which permits use, sharing, adaptation, distribution and reproduction in any medium or format, as long as you give appropriate credit to the original author(s) and the source, provide a link to the Creative Commons license, and indicate if changes were made. The images or other third party material in this article are included in the article's Creative Commons license, unless indicated otherwise in a credit line to the material. If material is not included in the article's Creative Commons license and your intended use is not permitted by statutory regulation or exceeds the permitted use, you will need to obtain permission directly from the copyright holder. To view a copy of this license, visit <http://creativecommons.org/licenses/by/4.0/>.

© The Author(s) 2019